

Biosorption of Methylene Blue from aqueous solution on spent cottonseed hull substrate for *Pleurotus ostreatus* cultivation

Qi Zhou^a, Wenqi Gong^{a*}, Chuanxin Xie^b, Xiao Yuan^a, Yubiao Li^a, Cuiping Bai^a, Shaohua Chen^a, Nian Xu^a

^aSchool of Resources and Environmental Engineering, Wuhan University of Technology, Wuhan 430070, PR China
Tel. +86 (27) 87372102; Fax +86 (27) 87882128; email: gongwenqi@yahoo.com.cn

^bSINOPEC Research Institute of Safety Engineering, Qingdao, 266071, PR China

Received 27 August 2010; Accepted in revised form 26 December 2010

ABSTRACT

The work presented in this paper focuses on studying the batch adsorption of a basic dye, Methylene Blue (MB), from aqueous solution onto the spent cottonseed hull substrate (SCHS) after used for *Pleurotus ostreatus* cultivation, in order to explore its potential use as a low-cost natural biosorbent for dye removal from wastewater. The biosorbent–MB interaction mechanism was investigated using a combination of FTIR and SEM techniques. Variables of the system, including solution pH, particle size, reaction time, SCHS dosage and initial MB concentration, were adjusted to study their effects on MB biosorption. The results showed that the kinetics of dye removal by SCHS was rapid, with 90.0% sorption within the first 5 min and equilibrium attained after 180 min. Biosorption kinetics and equilibrium followed the pseudo-second-order and Langmuir adsorption models. The maximum amount of MB adsorbed on SCHS was 185.22 mg/g. As a new adsorbent, experimental study showed that vast potential capacity for adsorbing MB existed in the SCHS.

Keywords: Spent cottonseed hull substrate (SCHS); *Pleurotus ostreatus*; Biosorption; Methylene Blue; Isotherm; Kinetics

1. Introduction

Synthetic dyes are used in many industries such as food, paper, carpets, rubbers, plastics, cosmetics, and textiles in order to color their products [1,2]. Colored water can affect plant life and thus an entire ecosystem can be destroyed by contamination from various dyes in water [3]. To avoid the environmental disaster engendered from the toxic chemical dyes, efficient and low-cost methods have to be developed to clean the industrial wastewater.

Methylene Blue (MB) is a thiazine (cationic) dye, which is most commonly used for coloring paper, temporary hair colorant, dyeing cottons, wools, etc. MB is not strongly hazardous, but it can cause some harmful effects. Many new biomaterials have been reported to remove MB, such as rice husk [4], hazelnut shells [1], spent coffee grounds [5], sawdust [6–8], peanut hull [9], wheat shells [10], softstem bulrush [11] and phoenix tree leaf powder [12], with large specific surface area. These biosorbents are composed basically of polysaccharide lignin, cellulose, hemicellulose and protein, containing plenty of binding sites, e.g. carboxyl, hydroxyl and amidogen, etc., which

* Corresponding author.

makes it possible for the bio-resources to adsorb ions from wastewater. Their high efficiency of biosorption and low costs attract people to exploit more bio-resources to alternate traditional processes.

Mushroom production industry is the biggest solid-state-fermentation industry in the world [13]. The spent mushroom substrate (SMS) is a bulky waste byproduct of the edible fungi production. SMS has been employed in recent years for different applications. However, most of these applications have been unable to solve the problem of its disposal completely, except its agricultural use as fertilizer [14]. Plenty of biomass species in SMS, made it more important benefits to human people, such as adsorbing cadmium, lead and chromium [15], and removing biocide pentachlorophenol [16], and spilled petroleum in industrial soils [17].

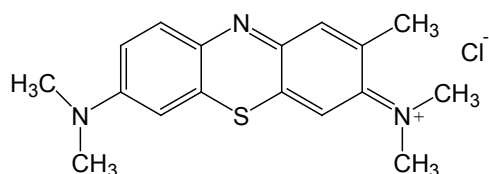
One of the popularly cultivated mushroom species worldwide belongs to the genus *Pleurotus ostreatus* (*P. ostreatus*). It can be cultivated on a wide range of substrates such as rice straw, corn stalk and cottonseed hull, wheat or oat straw, sawdust or combinations of these ingredients [18]. Previous research has shown that cottonseed hulls possess advantages as a substrate material due to its higher waterholding capability and nitrogen content. In China, *P. ostreatus* is often cultivated on cottonseed hulls as substrate. It was observed that the dry matter and cellulose, hemicellulose, lignin, and protein contents in cottonseed hull substrate changed considerably during *P. ostreatus* growing period. The total dry matter of cottonseed hull substrate decreased by nearly 50% after cultivation was completed [19], with increasing specific surface area. The spent substrate needs to be treated properly in order to minimize its possible adverse effects on the environment.

In this study, an attempt was made to use SCHS after *P. ostreatus* cultivation as an adsorbent to remove MB. Batch sorption experiments were carried out to study the feasibility. Results of this study will be useful for future scale up using as a low-cost biosorbent for the removal of cationic dyes from water.

2. Materials and methods

2.1. Solutions and reagents

Methylene Blue (MB, $C_{16}H_{18}N_3SCl_3 \cdot H_2O$, C.I. 52015, formula weight 373.90) was purchased from Tianjin Chemical Reagent Company (Tianjin, China). MB has the structure as follows:



The stock solution was prepared by dissolving accurately weighted MB in distilled water to the concentration of 400 mg/L. The working solutions were prepared by diluting the dye stock solution with distilled water to the required concentrations. Fresh dilutions were used for each adsorption study. The initial pH value of solution was adjusted with 0.10 mol/L NaOH or HCl solutions.

2.2. Preparation and characterization of biosorbent

The solid SCHS of *P. ostreatus* (2026) was kindly provided by the Pingdu Edible Fungi Ltd. (Shandong, China). The biomass was dried in an oven at 353 K for a period of 24 h, and then crushed in a knife-mill. The resulting material was screened through a set of sieves to get different geometrical sizes 120–830 μm . This produced a uniform material for the complete set of adsorption tests, which was then preserved in an airtight container and used in the adsorption studies.

The Fourier transform infrared (FTIR) spectroscopic technique was an important tool to identify some characteristic functional groups to prove that SCHS was capable of adsorbing MB. The FTIR spectra of MB, MB-loaded SCHS and SCHS were obtained using a FTIR Spectrometer (Thermo Nicolet, Nexus). Approximately 1 mg of sample ($\leq 2 \mu\text{m}$) was mixed with 100 mg KBr in order to prepare a translucent sample disk. Data analysis focused on the 400–4000 cm^{-1} region. The spectra were recorded with a resolution of 4 cm^{-1} .

The morphological characterization of the SCHS and MB-loaded SCHS samples were also analyzed to examine the surface morphology and structure of the biosorbent before and after MB sorption by scanning electron microscope (SEM), JSM-5610LV, using an acceleration voltage of 20 kV and magnification ranging from 500 to 10,000 times.

2.3. Adsorption experiments

The batch equilibrium process was used to characterize the biosorption ability of SCHS in a shaking water bath (Julabo SW23, Germany) at 150 rpm for a period of time at the temperature of 293 K. In each adsorption experiment, SCHS was added to 100 mL dye solution of known initial concentration in a 250 mL conical flask and the effect of pH values, particle sizes, reaction time, SCHS dosage and initial MB concentration were investigated to optimize the biosorption conditions. After shaking the flasks for predetermined time intervals, the samples were withdrawn from the flasks and the MB solutions were separated from the SCHS by filtration with stainless steel strainer, followed by centrifugation at 7,500 rpm for 10 min. The resulting solution was analyzed using a UV-Vis spectrophotometer (Agilent 8453, USA) by monitoring the absorbance at a wavelength of maximum absorbance (665 nm). The experiments were conducted in triplicate and the negative controls (with no biosorbent) were simultaneously carried out to ensure that biosorption was

by SCHS rather than the container. Following a systematic process, the biosorption uptake capacity of MB in batch system was tested in the present work.

The amount of MB adsorbed was calculated by subtracting the final solution concentration from the initial concentration. The amount of adsorbed MB per gram SCHS (q_e , mg/g) at equilibrium was obtained using the following equations:

$$q_e = \frac{V(C_0 - C_e)}{1000W} \quad (1)$$

$$p = \frac{C_0 - C_e}{C_0} \times 100 \quad (2)$$

where q_e is the equilibrium uptake value (the amount of MB adsorbed onto per unit mass of SCHS, mg/g), V is the sample volume (mL), C_0 is the initial MB concentration (mg/L), C_e is the equilibrium MB concentration (mg/L), W is the dry weight of the SCHS (g), and p is the removal efficiency (%).

3. Results and discussion

3.1. Characterization of SCHS

The biosorbent SCHS was characterized using a combination of FTIR and SEM techniques and the results are given in Figs. 1 and 2.

According to the FTIR spectra in Fig. 1, the broad absorption peak around 3407 cm^{-1} indicates the existence of bound hydroxyl groups (–OH), presumably contributed by the cellulosic cell wall. The two peaks at about 2920 and 2852 cm^{-1} , are attributed to the symmetric and asymmetric stretching of aliphatic C–H groups bound by the stretching of the –OH groups. The peak at 1645 cm^{-1} was the characteristics of C=O bonds in aldehydes, ketones or carboxylic acids. In addition to these, a sharp and narrow peak located at 1324 cm^{-1} probably indicates the presence of C–O bonds in alcohols or carboxylic acids. These FTIR results indicate that there were functional groups such as –OH, COO^- and C=O in the biosorbent SCHS, which could be potential adsorption sites for interaction with MB.

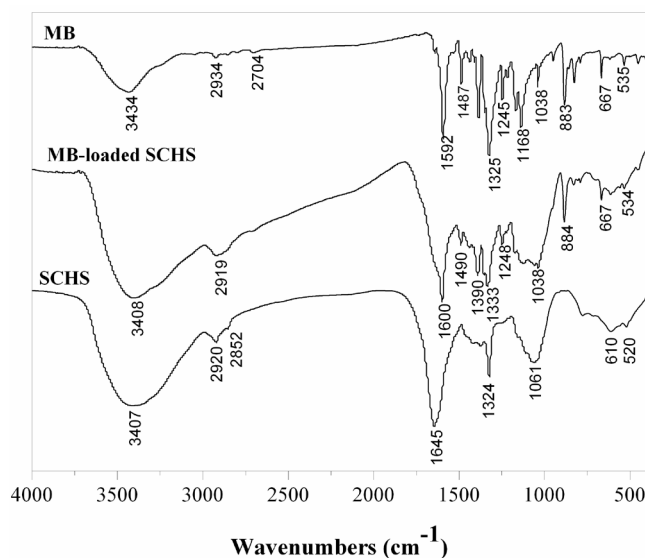


Fig. 1. FTIR spectrograms of MB, MB-loaded SCHS and SCHS.

Comparing the FTIR spectra of three samples in Fig. 1, the peak at 884 cm^{-1} of MB-loaded SCHS spectrum can be assigned to the δ -CH out-of-plane bending in the aromatic ring of MB, the two peaks at 1600 and 1490 cm^{-1} are the characteristics of the skeleton ring stretching absorption of MB indole ring (benzo-N hybrid five-membered ring). The other significant changes between unloaded and loaded SCHS can be found by some characteristic absorption peaks at 1248, 1038, 790, 667, 534 cm^{-1} , which indicate probably the presence of MB in MB-loaded SCHS. Finally, the obvious difference is the vibration frequency of $-\text{COO}^-$ groups. It is observed that the related absorption band has shifted from 1418 to 1385 cm^{-1} . A shift in a frequency relates to an energy change of the functional group and this indicates that the bonding pattern of carbonyl groups changed after biosorption [20].

The surface morphology of the biosorbent before and after MB biosorption was evaluated by scanning electron microscopy (SEM) in this work. SEM images of unloaded and MB-loaded SCHS at 1000 times of magnification are

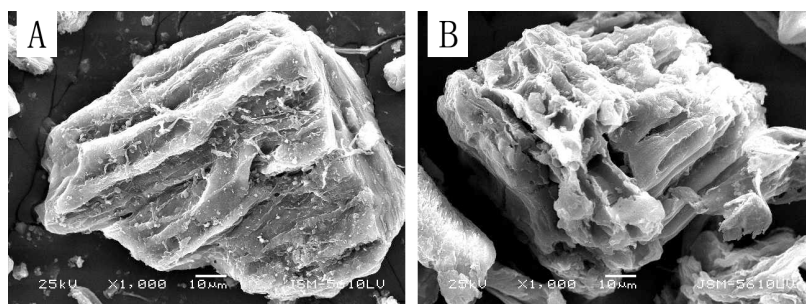


Fig. 2. SEM micrographs of (A) unloaded and (B) MB-loaded SCHS.

shown in Fig. 2. These micrographs show the fibrous structure of unloaded and MB-loaded SCHS. Some holes and cavities in these fibers can be seen, which indicate the presence of microporous and irregular inner structure, which made it possible for MB to adsorb on the vast different surface of the biosorbent. After the biosorption process, the surface structure of SCHS slightly changed which appears to be rough. New shiny particles looking like sponge on the uneven surface of the sample may be attributed to the coverage of the surface by a layer of MB. Similar result was also observed by Akar [20].

3.2. Influence of solution pH on biosorption

pH was one of the most important parameters on biosorption of MB from aqueous solutions, and the results are shown in Fig. 3.

From Fig. 3, it is observed that the solution pH affects the values of removal efficiency (p %) which increase significantly with increasing pH ranging from 2.0 up to 5.0. The adsorption quantity reaches a maximum level at the pH of 10.0, but the uptake capacity does not change significantly from 6.0 to pH 10.0 and the amount of dye removal is kept practically constant (variations lower than 1.2%). The highest biosorption capacity of MB by the SCHS is 77.75 mg g^{-1} at pH 10. Several reasons may be attributed to the MB adsorption behavior on the biosorbent relative to solution pH. The surface of SCHS may contain a large number of active sites and the solute uptake (MB ions) can be related to the active sites. At lower pH, the surface of biosorbent would also be surrounded by the excess hydronium ions, which competed with MB cations for active biosorption sites [20]. At higher pH the surface of SCHS particles may become negatively charged, which enhanced the positively charged dye cations through

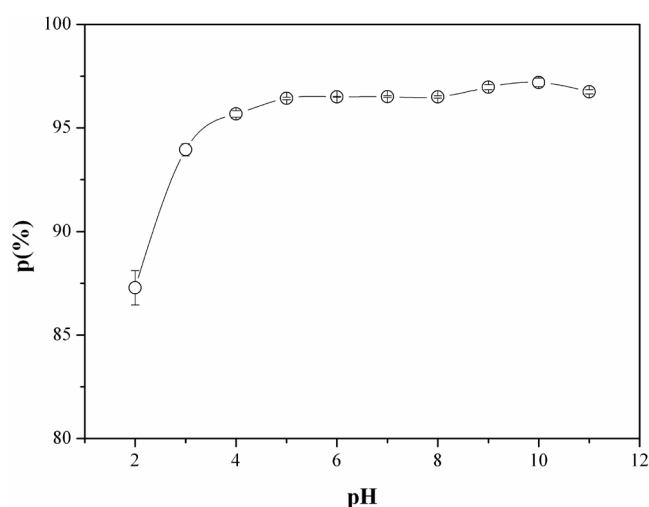


Fig. 3. Influence of solution pH on biosorption MB by SCHS (reaction time 180 min, MB concentration 200 mg/L, SCHS dosage 2.5 g/L, particle size 120–150 μm , temperature 293 K).

electrostatic forces of attraction. From the above FTIR spectra it can be seen that many functional groups such as hydroxyl and carboxylic acids exist on the surface of the SCHS. The electrostatic attraction between the positively charged MB ions and the negative surface of the SCHS increased with pH. The results in the stronger biosorption ability were observed when pH of the solution increased.

3.3. Influence of particle size on biosorption

Adsorption of MB dye on SCHS of six different particle sizes (<120, 120–150, 150–180, 180–250, 250–380, 380–830 μm) was studied keeping the other parameters as constant. Fig. 4 shows the influence of biosorbent particle size on removal efficiency (%) of MB.

From Fig. 4, it can be observed that as the particle size decreases, the biosorption of the dye increases. The adsorption ratios of MB has approached the maximum values when the biosorbent particle size was in the range of 120–150 μm , which was due to larger surface area associated with smaller particles. For larger particles, the diffusion resistance to mass transport was higher and most of the internal surface of the particles may not be used for biosorption and consequently, the amount of MB adsorbed was small. It was also observed that as the particle size decreased, the dye uptake, which was the amount of dye adsorbed on the particles increased [1]. For convenience of liquid–solid phase separation, the biosorbent particle of 120–150 μm was utilized in all other parameter experiments.

3.4. Influence of SCHS dosage on biosorption

In order to make clear the least SCHS dosage for a maximal removal of MB, the dosage effect of SCHS was examined. And the results are shown in Fig. 5.

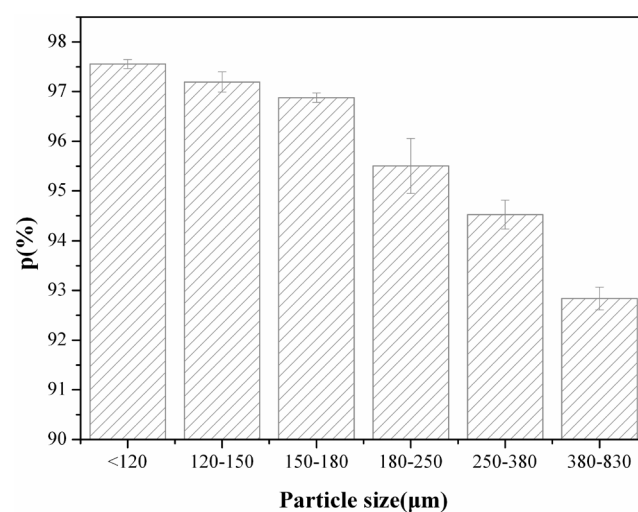


Fig. 4. MB removal percentages with SCHS of different particle sizes (reaction time 180 min, MB concentration 200 mg/L, SCHS dosage 2.5 g/L, pH 10.0, temperature 293 K).

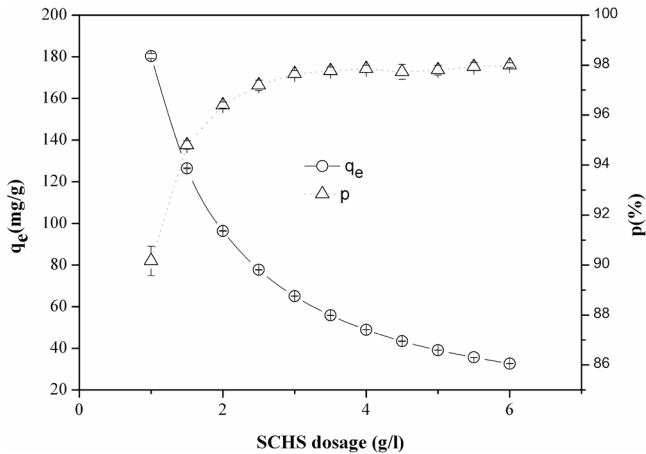


Fig. 5. Influence of SCHS dosage on biosorption and removal efficiency of MB (reaction time 180 min, MB concentration 200 mg/L, particle size 120–150 μm , pH 10.0, temperature 293 K).

As shown in Fig. 5, the biosorption of MB increases with the biosorbent dosage. It is observed that the percent removal efficiency of MB increases from 90.17% to 98.00% when the biosorbent dosage increases from 1.0 to 6.0 g/L. On the other hand, the plot of biosorption amount vs. the biosorbent dosage shows that with increasing the SCHS dosage from 1.0 to 6.0 g/L, the value of q_e decreases from 180.34 to 32.67 mg/g.

When the dosage of the biosorbent is more than 3.0 g/L, the curve of removal efficiency (p %) reaches a plateau. The highest adsorption capacity occurred in the lowest biomass dosage of 1.0 g/L with the adsorption capacity of 180.34 mg/g for MB. Other adsorbent, such as hazelnut shells [1], rice husk [4], fallen phoenix tree's leaves [2], had similar results about the dosage effect on MB adsorption. The primary factor explaining this characteristic was that adsorption sites remained unsaturated during the adsorption reaction, whereas the number of sites available for adsorption increased by increasing the SCHS dosage. As the value of removal percentages (p) was 97.19% at the SCHS dosage of 2.5 g/L, this dosage was adopted in the present study.

3.5. Influence of reaction time on biosorption and kinetics modeling

The biosorption data for the uptake capacity of biosorption quantity per gram SCHS (q_t , mg/g) vs. reaction time are shown in Fig. 6.

In the wastewater treatment processes the equilibrium time between the dye molecules and the biosorbent is of significant importance [20]. As shown in Fig. 6, the biosorption capacity of biomass increases instantly and reaches a high value at the initial stages (within 5 min) of the contact period. A large number of vacant sites on the

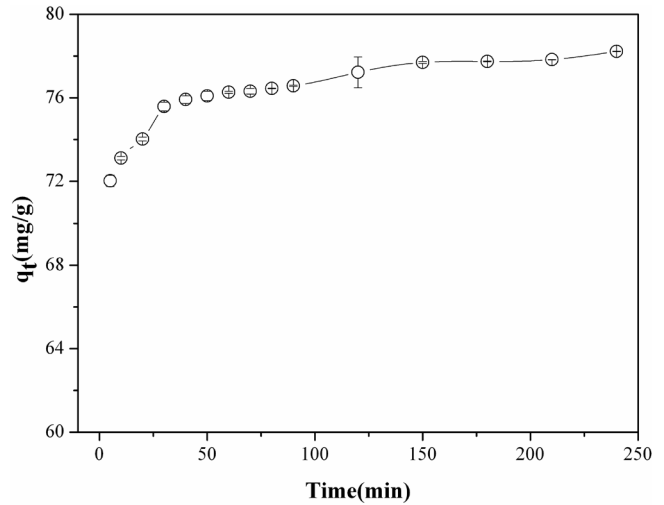


Fig. 6. Influence of reaction time on biosorption of MB on SCHS (MB concentration 200 mg/L, SCHS dosage 2.5 g/L, particle size 120–150 μm , pH 10.0, temperature 293 K).

SCHS surface are available during the biosorption at this stage. Thereafter, it becomes slower near the biosorption equilibrium and the maximum removal of MB occurs within 180 min. After this period the amount of adsorbed MB does not significantly change with time due to the repulsive forces between the MB molecules on the solid and bulk phases and this trend indicates that the biosorbent is saturated with the adsorbate at this level. According to the results of the experiments, the reaction time was fixed at 180 min for the rest of the batch experiments to make sure that equilibrium was reached.

Kinetic studies have been carried out to determine the time required to attain the biosorption equilibrium and the efficiency of MB biosorption onto biomass. Table 1 shows the predicted equations for the three important kinetic models which were chosen to analyze the kinetic behavior of SCHS in this study. Fig. 7 and Fig. 8 were fitted to describe the adsorption process of MB on SCHS with the three kinetic models [18,21–25] according to Table 1 and the experimental data in 180 min.

From Fig. 7, a straight line of $\ln(q_e - q_t)$ vs. t would suggest that this kinetic model is applicable to the data tested, and k_1 and q_e are determined from the slope and intercept of the plot, respectively. But it is found that the kinetic data obtained from this equation does not follow the pseudo-first-order model for the biosorption of MB onto SCHS.

According to Fig. 7, pseudo-second-order could well fit the test data. The pseudo-second-order kinetic model with R^2 value of 0.999 showed good agreement with the experimental values. The values of k_2 and q_t were calculated from a plot of t/q_t vs. t . The predicted equilibrium adsorption capacities (q_e) by pseudo-second-order

Table 1
Kinetic equations

Kinetic model	Equation	Kinetic constants
Pseudo-first-order	$\ln(q_e - q_t) = \ln q_e - k_1 t$	q_t (mg/g) is the amount of solute adsorbed per gram of adsorbent over a time period t (min), and k_1 (min^{-1}) the first-order kinetic constant
Pseudo-second-order	$\frac{t}{q_t} = \frac{1}{k_2 q_e^2} + \frac{t}{q_e}$	k_2 ($\text{g mg}^{-1} \text{min}^{-1}$) is the second-order kinetic constant
Intraparticle diffusion	$q_t = k_p t^{1/2} + C$	k_p ($\text{g mg}^{-1} \text{min}^{-1}$) is the constant of intraparticle diffusion, C is the intercept

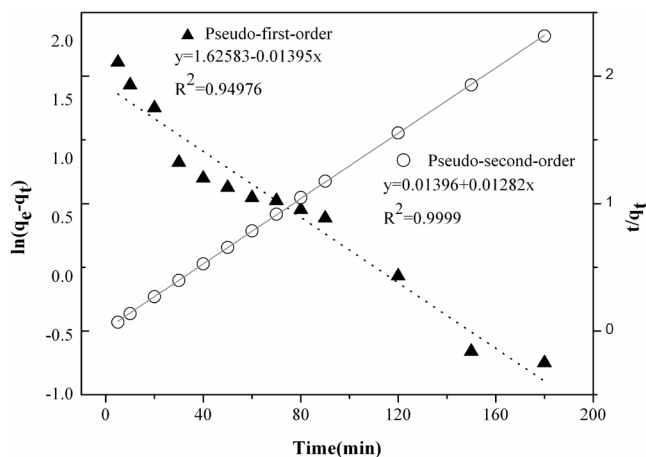


Fig. 7. Pseudo-first-order and pseudo-second-order kinetic functions of the biosorption of MB onto SCHS.

kinetics is 78.00312 mg/g for solutions with initial MB concentrations at 200 mg/L. The kinetic model constants k_2 is 0.01178.

The intraparticle diffusion model is based on the transfer of matter from the external surface to the surface inside the pores [26]. By the plots of q_t vs. $t^{1/2}$ of MB, multilinearities were observed in Fig. 8, indicating that three steps took place. The first sharper portion was attributed to the diffusion of MB through the solution to the external surface of adsorbent, or the boundary layer diffusion of solute molecules. The second portion described the gradual adsorption stage, where intraparticle diffusion was rate limiting. The third portion was attributed to the final equilibrium stage for which the intraparticle diffusion started to slow down due to the extremely low dye concentration left in the solution. The rate of uptake might be limited by the size of the adsorbate molecule, concentration of the adsorbate and its affinity to the adsorbent, diffusion coefficient of MB in the bulk phase, and the pore-size distribution of the adsorbent [27].

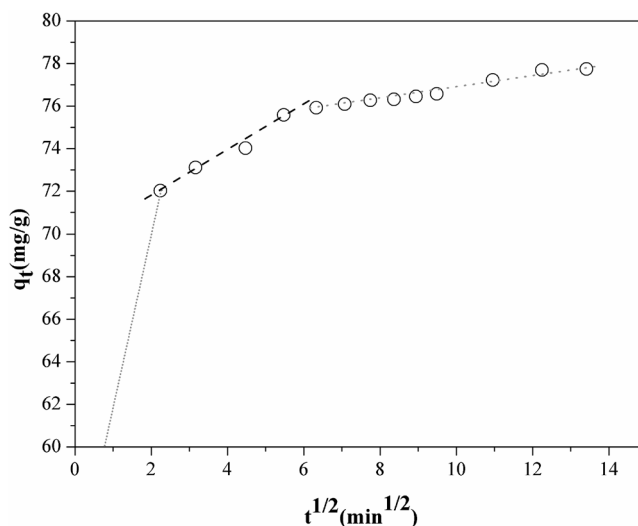


Fig. 8. Intraparticle diffusion plots for the biosorption of MB onto SCHS.

As seen from Fig. 8, the plots were not linear over the whole time range, implying that more than one process affected the adsorption. The multiple natures of these plots could be explained by boundary layer diffusion, which gave the first portion and the intraparticle diffusion that produced the further two linear portions. If the intraparticle diffusion was the only rate-controlling step, the plot passed through the origin; if not, the boundary layer diffusion controlled the adsorption to some degree. It could be deduced that there were three processes that controlled the rate of molecules adsorption but only one was rate limiting in any particular time range. The slope of the linear portion indicated the rate of the adsorption. The lower slope corresponded to a slower adsorption process. One could observe that the diffusion in bulk phase to the exterior surface of adsorbent, which started at the onset of the process, was the fastest. The second portion of the plot seemed to refer to the diffusion into mesopores and

the third one with the lowest slope to adsorption into micropores. This implied that the intraparticle diffusion of dye molecules into micropores was the rate-limiting step in the adsorption process on SCHS, particularly over long contact time periods [27].

3.6. Influence of initial MB concentration on biosorption

The results about the influence of the initial MB concentration on biosorption are shown in Fig. 9.

As shown in Fig. 9, the percent removal efficiency of MB decreases from 98.11% to 84.11% when the initial concentration increases from 50 to 500 mg/L. But the equilibrium MB concentration (C_e) increases with increasing initial MB concentrations at the range of experimental concentration. Under the same conditions, if the concentration of MB in solution was bigger, the active sites of SCHS were surrounded by much more MB ions, and the process of adsorption would proceed more sufficiently, but the equilibrium concentration would increase. So the values of C_e and q_e increased with increasing initial MB concentrations.

3.7. Determination of adsorption isotherm model constants about MB/SCHS system

The analysis of biosorption process requires equilibrium to better understand the adsorption process. Equilibrium isotherm equations are used to describe the experimental sorption data [2]. In this work, the equilibrium models were fitted employing the linear fitting method using the software Microcal Origin 8.0.

At equilibrium, a dynamic equilibrium was established in the concentration of sorbate between two phases.

The equilibrium isotherm was of fundamental importance for the design and optimization of the adsorption system for the removal of MB from aqueous solution. Therefore, it is necessary to establish the most appropriate correlation for the equilibrium curves. In the present study, Langmuir and Freundlich equilibrium models have been applied [1,28–30].

The Langmuir adsorption isotherm has been successfully applied to many pollutants sorption processes and is the most widely used sorption isotherm for the sorption of a solute from a liquid solution. A basic assumption of the Langmuir theory is that sorption takes place at specific homogeneous sites within the adsorbent. The saturated monolayer isotherm can be represented as:

$$q_e = \frac{q_{\max} K_L C_e}{1 + K_L C_e} \quad (3)$$

where q_{\max} and K_L are the Langmuir model constants. These constants are called the adsorption capacity (maximum surface coverage) and bonding energy constant, respectively. The Langmuir adsorption isotherm has traditionally been used to quantify and contrast the performance of different sorbents. It has served to estimate the maximum dye uptake values where they could not be reached in the experiments [31].

The Freundlich isotherm is an empirical expression that encompasses the heterogeneity of the surface and an exponential distribution of the sites and their energies. This isotherm has been further extended by considering the influence of adsorption sites and the competition between different adsorbents for adsorption on the available sites. Freundlich isotherm has been observed for a wide range of heterogeneous surfaces including activated carbon, silica, clays, and polymers. The Freundlich equation can be written as:

$$q_e = K_F C_e^{1/n} \quad (4)$$

where $1/n$ is the heterogeneity factor of the adsorbent and K_F is constant. The surface heterogeneity is due to the existence of crystal edges, type of cations, surface charges, surface modification groups, and degree of crystallinity of the surface. The $1/n$ value indicates the relative distribution of energy sites and depends on the nature and strength of the adsorption process.

In the present study, model constants were determined using non-linear regression analysis of the batch biosorption data in Fig. 9 as described in Eqs. (3) and (4). The comparisons between experimental data and theoretical plots of Langmuir and Freundlich isotherm models, the model constants, along with their correlation coefficients (R^2) for biosorption of MB onto SCHS, are presented in Fig. 10.

Fig. 10 shows the model constants along with correlation coefficients for biosorption of MB onto SCHS. For the Freundlich model, correlation coefficient R^2 was

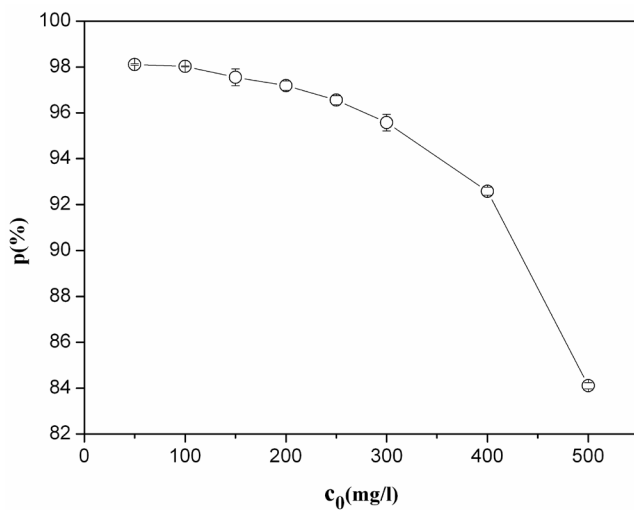


Fig. 9. Equilibrium adsorption quantities of MB at different initial concentrations (reaction time 180 min, SCHS dosage 2.5 g/L, particle size 120–150 μm , pH 10.0, temperature 293 K).

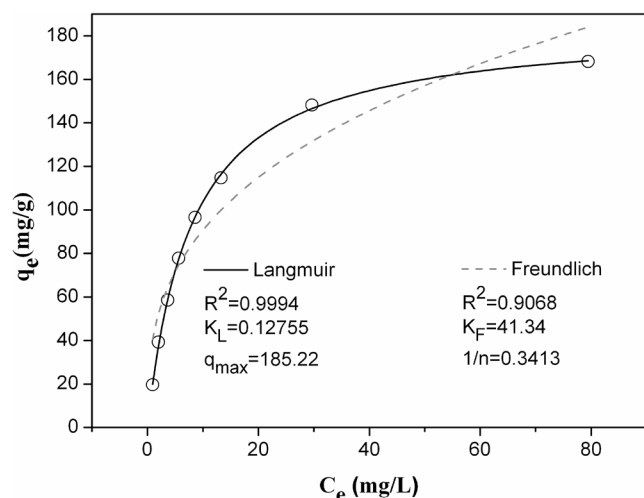


Fig. 10. Langmuir and Freundlich adsorption isotherms of MB on SCHS.

0.9068, while the R^2 for Langmuir model was 0.9994. The comparison of correlation coefficients (R^2) of the nonlinearized form of both equations indicates that the Langmuir model yielded a better fit for the experimental equilibrium adsorption data than the Freundlich model. This suggests the Langmuir monolayer coverage of the surface of SCHS by MB molecules, which may be associated with the homogeneous surface of the SCHS.

Although the model could not provide mechanistic information of the sorption phenomena, it might be used to estimate the maximum uptake of MB (q_{\max}). From the experimental data, the q_{\max} of the estimated Langmuir parameters for MB biosorption are shown in Table 2.

The maximum uptake (q_{\max}) of MB is 185.22 mg/g, which is much greater than some other biosorbents described in Table 1. The q_{\max} values show that the biosorp-

Table 2
MB adsorption by different biosorbents: q_{\max} of various related substances from the Langmuir constant

Biosorbent	q_{\max} (mg/g)	Reference
Rattan sawdust	294.14	[32]
Jackfruit peel	285.71	[33]
SCHS of <i>P. ostreatus</i>	185.22	This study
<i>Pyracantha coccinea</i> berries	127.50	[20]
Fallen phoenix tree's leaves	89.70	[2]
Tea waste	85.16	[34]
Hazelnut shells	80.01	[1]
Softstem bulrush	53.8	[11]
Yellow passion fruit waste	44.70	[35]
Rice husk	40.58	[36]

tion capacity of SCHS particles is highly comparable to that of some other low-cost adsorbent materials for MB. As a kind of solid waste, SCHS is plenty and cheap, and thus can be used to remove MB from wastewater.

4. Conclusions

The biosorption of MB from aqueous solution by SCHS as adsorbent has been investigated under different experimental conditions in batch mode. The values of q_e about MB adsorbed onto SCHS were dependent on the solution pH, particle size, reaction time, SCHS dosage, and MB initial concentration. The MB adsorption processes on SCHS followed the pseudo-second order rate kinetics. The equilibrium data were found to be better represented by the Langmuir isotherm model according to the linear regressive analysis. The maximum amount of MB adsorbed on SCHS was 185.22 mg/g. The functional groups on the biosorbent surface such as hydroxyl and carboxyl were found to play a role in the biosorption process according to the infrared spectroscopic analysis of the SCHS. As a common edible fungus in China, *P. ostreatus* cultivation spent substrate is a locally available and low-cost material in the countryside at zero or negligible price. Therefore, SCHS can be used as a biosorbent for the removal of the cationic dye MB from dilute industrial effluents, without any laborious pretreatment steps before application.

Acknowledgements

This work was financially supported by the self-determined and innovative research funds of Wuhan University of Technology (2010-YB-16), Hubei Provincial Key Laboratory of Pollutant Analysis and Reuse Technology Open Fund Project (No. KY 2010G 19) and National Natural Science Foundation of China (No.50802066).

References

- [1] M. Dogan, H. Abak and M. Alkan, Biosorption of methylene blue from aqueous solutions by hazelnut shells: Equilibrium, parameters and isotherms, *Water Air Soil Pollut.*, 192 (2008) 141–153.
- [2] R.P. Han, W.H. Zou, W.H. Yu, S.J. Cheng, Y.F. Wang and J. Shi, Biosorption of methylene blue from aqueous solution by fallen phoenix tree's leaves, *J. Hazard. Mater.*, 141 (2007) 156–162.
- [3] S.B. Wang, Z.H. Zhu, A. Coomes, F. Haghseresht and G.Q. Lu, The physical and surface chemical characteristics of activated carbons and the adsorption of methylene blue from wastewater, *J. Colloid Interf. Sci.*, 284 (2005) 440–446.
- [4] R.P. Han, Y.F. Wang, W.H. Yu, W.H. Zou, H. Shi and H.M. Liu, Biosorption of methylene blue from aqueous solution by rice husk in a fixed-bed column, *J. Hazard. Mater.*, 141 (2007) 713–718.
- [5] A.S. Franca, L.S. Oliveira and M.E. Ferreira, Kinetics and equilibrium studies of methylene blue adsorption by spent coffee grounds, *Desalination*, 249 (2009) 267–272.
- [6] V.K. Garg, M. Amita, R. Kumar and R. Gupta, Basic dye (methylene blue) removal from simulated wastewater by adsorption sawdust: a timber using Indian Rosewood industry waste, *Dyes Pigments*, 63 (2004) 243–250.

- [7] A.E. Ofomaja, Equilibrium sorption of Methylene Blue using mansonia wood sawdust as biosorbent, *Desal. Wat. Treat.*, 3 (2009) 1–10.
- [8] M.M.A. El-Latif and A.M. Ibrahim, Adsorption, kinetic and equilibrium studies on removal of basic dye from aqueous solutions using hydrolyzed oak sawdust, *Desal. Wat. Treat.*, 6 (2009) 252–268.
- [9] R.M. Gong, M. Li, C. Yang, Y.Z. Sun and J. Chen, Removal of cationic dyes from aqueous solution by adsorption on peanut hull, *J. Hazard. Mater.*, 121 (2005) 247–250.
- [10] Y. Bulut and H. Aydin, A kinetics and thermodynamics study of Methylene Blue adsorption on wheat shells, *Desalination*, 194 (2006) 259–267.
- [11] Y. Li, J. Zhang, C.L. Zhang, L. Wang and B. Zhang, Biosorption of Methylene Blue from aqueous solution by softstem bulrush (*Scirpus tabernaemontani* Gmel.), *J. Chem. Technol. Biotechnol.*, 83 (2008) 1639–1647.
- [12] R.P. Han, Y. Wang, X. Zhao, Y.F. Wang, F.L. Xie, J.M. Cheng and M.S. Tang, Adsorption of Methylene Blue by phoenix tree leaf powder in a fixed-bed column: Experiments and prediction of breakthrough curves, *Desalination*, 245 (2009) 284–297.
- [13] K.L. Lau, Y.Y. Tsang and S.W. Chiu, Use of spent mushroom compost to bioremediate PAH-contaminated samples, *Chemosphere*, 52 (2003) 1539–1546.
- [14] C. Paredes, E. Medina, R. Moral, M.D. Perez-Murcia, J. Moreno-Caselles, M.A. Bustamante and J.A. Cecilia, Characterization of the different organic matter fractions of spent mushroom substrate, *Commun. Soil Sci. Plant Anal.*, 40 (2009) 150–161.
- [15] G.Q. Chen, G.M. Zeng, X. Tu, G.H. Huang and Y.N. Chen, A novel biosorbent: characterization of the spent mushroom compost and its application for removal of heavy metals, *J. Environ. Sci. – China*, 17 (2005) 756–760.
- [16] W.M. Law, W.N. Lau, K.L. Lo, L.M. Wai and S.W. Chiu, Removal of biocide pentachlorophenol in water system by the spent mushroom compost of *Pleurotus pulmonarius*, *Chemosphere*, 52 (2003) 1531–1537.
- [17] S.W. Chiu, T. Gao, C.S.S. Chan and C.K.M. Ho, Removal of spilled petroleum in industrial soils by spent compost of mushroom *Pleurotus pulmonarius*, *Chemosphere*, 75 (2009) 837–842.
- [18] Q. Zhou, W. Gong, C. Xie, D. Yang, X. Ling, X. Yuan, S. Chen and X. Liu, Removal of Neutral Red from aqueous solution by adsorption on spent cottonseed hull substrate, *J. Hazard. Mater.*, 185 (2011) 502–506.
- [19] X. Li, Y. Pang and R. Zhang, Compositional changes of cottonseed hull substrate during *P. ostreatus* growth and the effects on the feeding value of the spent substrate, *Bioresour. Technol.*, 80 (2001) 157–161.
- [20] T. Akar, B. Anilan, A. Gorgulu and S.T. Akar, Assessment of cationic dye biosorption characteristics of untreated and non-conventional biomass: *Pyracantha coccinea* berries, *J. Hazard. Mater.*, 168 (2009) 1302–1309.
- [21] M.F. Zhao and P. Liu, Adsorption of Methylene Blue from aqueous solutions by modified expanded graphite powder, *Desalination*, 249 (2009) 331–336.
- [22] D.A. Fungaro, M. Bruno and L.C. Grosche, Adsorption and kinetic studies of Methylene Blue on zeolite synthesized from fly ash, *Desal. Wat. Treat.*, 2 (2009) 231–239.
- [23] W.H. Zou, P. Han, Y.L. Lia, X. Liu, X.T. He and R.P. Han, Equilibrium, kinetic and mechanism study for the adsorption of Neutral Red onto rice husk, *Desal. Wat. Treat.*, 12 (2009) 210–218.
- [24] A.S. Franca, L.S. Oliveira, S.A. Saldanha, P.I.A. Santos and S.S. Salum, Malachite green adsorption by mango (*Mangifera indica* L.) seed husks: Kinetic, equilibrium and thermodynamic studies, *Desal. Wat. Treat.*, 19 (2010) 241–248.
- [25] L. Khenniche and F. Aissani, Characterization and utilization of activated carbons prepared from coffee residue for adsorptive removal of salicylic acid and phenol: Kinetic and isotherm study, *Desal. Wat. Treat.*, 11 (2009) 192–203.
- [26] Z. Li, X. Tang, Y. Chen, L. Wei and Y. Wang, Activation of *Firmiana simplex* leaf and the enhanced Pb(II) adsorption performance: equilibrium and kinetic studies, *J. Hazard. Mater.*, 169 (2009) 386–394.
- [27] W.H. Cheung, Y.S. Szeto and G. McKay, Intraparticle diffusion processes during acid dye adsorption onto chitosan, *Bioresour. Technol.*, 98 (2007) 2897–2904.
- [28] B.H. Hameed, A.T.M. Din and A.L. Ahmad, Adsorption of Methylene Blue onto bamboo-based activated carbon: Kinetics and equilibrium studies, *J. Hazard. Mater.*, 141 (2007) 819–825.
- [29] O.S. Bello, I.A. Adeogun, J.C. Ajaelu and E.O. Fehintola, Adsorption of Methylene Blue onto activated carbon derived from periwinkle shells: kinetics and equilibrium studies, *Chem. Ecol.*, 24 (2008) 285–295.
- [30] M.M. Abd El-Latif and A.M. Ibrahim, Removal of reactive dye from aqueous solutions by adsorption onto activated carbons prepared from oak sawdust, *Desal. Wat. Treat.*, 20 (2010) 102–113.
- [31] K. Vijayaraghavan, S.W. Won, J. Mao and Y.S. Yun, Chemical modification of *Corynebacterium glutamicum* to improve methylene blue biosorption, *Chem. Eng. J.*, 145 (2008) 1–6.
- [32] B.H. Hameed, A.L. Ahmad and K.N.A. Latiff, Adsorption of basic dye (Methylene Blue) onto activated carbon prepared from rattan sawdust, *Dyes Pigments*, 75 (2007) 143–149.
- [33] B.H. Hameed, Removal of cationic dye from aqueous solution using jackfruit peel as non-conventional low-cost adsorbent, *J. Hazard. Mater.*, 162 (2009) 344–350.
- [34] M.T. Uddin, M.A. Islam, S. Mahmud and M. Rukanuzzaman, Adsorptive removal of Methylene Blue by tea waste, *J. Hazard. Mater.*, 164 (2009) 53–60.
- [35] F.A. Pavan, E.C. Lima, S.L.P. Dias and A.C. Mazzocato, Methylene Blue biosorption from aqueous solutions by yellow passion fruit waste, *J. Hazard. Mater.*, 150 (2008) 703–712.
- [36] V. Vadivelan and K.V. Kumar, Equilibrium, kinetics, mechanism, and process design for the sorption of Methylene Blue onto rice husk, *J. Colloid Interf. Sci.*, 286 (2005) 90–100.